

## Molecular Recognition of Trigonal Oxyanions Using a Ditopic Salt Receptor: Evidence for Anisotropic Shielding Surface around Nitrate Anion

Joseph M. Mahoney,<sup>†</sup> Kenneth A. Stucker,<sup>†</sup> Hua Jiang,<sup>†</sup> Ian Carmichael,<sup>‡</sup>  
Nicole R. Brinkmann,<sup>‡</sup> Alicia M. Beatty,<sup>†</sup> Bruce C. Noll,<sup>†</sup> and Bradley D. Smith<sup>\*,†</sup>

Contribution from the Department of Chemistry and Biochemistry, and Radiation Laboratory,  
University of Notre Dame, Notre Dame, Indiana 46556-5670

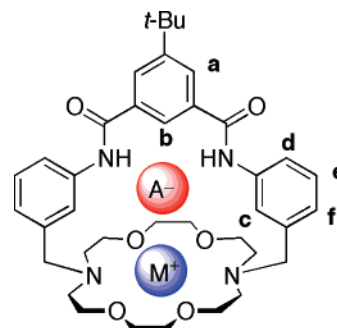
Received September 30, 2004; E-mail: smith.115@nd.edu

**Abstract:** A ditopic, macrobicyclic receptor with adjacent anion and cation binding sites is able to extract a range of monovalent salts into chloroform solution. The structures of the receptor complexed with KAcO, LiNO<sub>3</sub>, NaNO<sub>3</sub>, KNO<sub>3</sub>, and NaNO<sub>2</sub> are characterized in solution by NMR spectroscopy and in the solid state by X-ray crystallography. The sodium and potassium salts are bound to the receptor as contact ion-pairs, with the metal cation located in the receptor's crown ether ring and the trigonal oxyanion hydrogen bonded to the receptor NH residues. The solid-state structure of the LiNO<sub>3</sub> complex has a bridging water molecule between the cation and anion. In all solid-state structures, the trigonal oxyanion is not located symmetrically inside the receptor cavity. It appears that anion orientation is controlled by a complex interplay of steric factors, coordination bonding to the metal cation, and hydrogen bonding with the receptor NH residues. An important feature with this latter effect is the fact that hydrogen bonds directed toward the oxygen lone pairs on a trigonal oxyanion are stronger than hydrogen bonds to the  $\pi$ -electrons. In solution, the <sup>1</sup>H NMR spectra of the nitrate and nitrite salt complexes are noteworthy because several receptor signals, including the NH protons, undergo unusual upfield movements in chemical shift upon complexation. This is a reflection of the diamagnetic anisotropy of these trigonal oxyanions. The magnetic shielding surface for the NO<sub>3</sub><sup>-</sup> anion is calculated using density functional theory and shown to have a shielding region directly above the central nitrogen.

### Introduction

The structure and reactivity of ion-pairs has been a major chemical research topic for many decades; however, experimental studies have been complicated by the inherent high lability of the ion-pairs.<sup>1</sup> Our research group has designed several ditopic receptors that can bind and solubilize discrete ion-pairs in nonpolar solvents.<sup>2–4</sup> In particular, we recently reported that macrobicyclic receptor **1** can extract alkali halides into chloroform solution as associated ion-pairs (Scheme 1).<sup>3</sup> The signals for free receptor and receptor/salt complex exchange slowly on

Scheme 1. Receptor **1** with Bound Salt



the NMR chemical shift time scale, which means that the structures of the complexes are amenable to direct characterization by NMR. Moreover, the receptor/salt complexes can be readily recrystallized, which allows structural analysis by single-crystal X-ray diffraction. Since alkali metal cations (M) and halide anions (A) are both spherical ions, the assessment of structural complementarity that any receptor (R) has for an alkali halide contact ion-pair (MA) is relatively straightforward and primarily involves a consideration of R...A, R...M, and M...A distances. In this present contribution, we consider a more difficult recognition problem, namely, the ability of receptor **1** to bind contact ion-pairs that contain a trigonal oxyanion. In this case, the assessment of structural complementarity is more

<sup>†</sup> Department of Chemistry and Biochemistry.

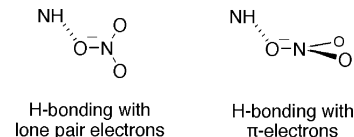
<sup>‡</sup> Radiation Laboratory.

- (1) Smid, J. *Angew. Chem., Int. Ed.* **1972**, *11*, 112–127. (b) Szczygiel, P.; Shamsipur, M.; Hallenga, K.; Popov, A. I. *J. Phys. Chem.* **1987**, *91*, 1255–1259. (c) Loupy, A.; Tchouber, B. *Salt Effects in Organic and Organometallic Chemistry*; VCH: Weinheim, Germany, 1992. (d) Mizoguchi, A.; Ohshima, Y.; Endo, Y. *J. Am. Chem. Soc.* **2003**, *125*, 1716–1717. (e) Das, A.; Tembe, B. L. *J. Chem. Phys.* **1998**, *108*, 2930–2939.
- (2) Shukla, R.; Kida, T.; Smith, B. D. *Org. Lett.* **2000**, *2*, 3039–3248. (b) Deetz, M. J.; Shang, M.; Smith, B. D. *J. Am. Chem. Soc.* **2000**, *122*, 6201–6207. (c) Mahoney, J. M.; Marshall, R. A.; Beatty, A. M.; Smith, B. D.; Camiolo, S.; Gale, P. A. *J. Supramol. Chem.* **2001**, *1*, 289–292. (d) Koulov, A. V.; Mahoney, J. M.; Beatty, A. M.; Smith, B. D. *Org. Biomol. Chem.* **2003**, *1*, 27–29. (e) Mahoney, J. M.; Davis, J. P.; Smith, B. D. *J. Org. Chem.* **2003**, *68*, 9819–6820.
- (3) Mahoney, J. M.; Beatty, A. M.; Smith, B. D. *J. Am. Chem. Soc.* **2001**, *123*, 5847–5848. (b) Mahoney, J. M.; Nawaratna, G. U.; Beatty, A. M.; Duggan, P. J.; Smith, B. D. *Inorg. Chem.* **2004**, *43*, 5902–5907. (c) Mahoney, J. M.; Beatty, A. M.; Smith, B. D. *Inorg. Chem.* **2004**, *43*, 7617–7621.

challenging because it requires consideration of the anisotropic shape of the anion and directionality of the noncovalent interactions.

We describe how receptor **1** forms complexes with alkali metal  $\text{AcO}^-$ ,  $\text{NO}_3^-$ , and  $\text{NO}_2^-$  salts. We investigate how these trigonal oxyanions, with lone pair and  $\pi$ -electron density, simultaneously interact with the NH residues on receptor **1** and the bound alkali metal cation. The degree that  $\pi$ -electrons are involved in noncovalent interactions is a fundamental question that dates back many decades to studies of electron donor–acceptor complexation.<sup>5</sup> The context here is somewhat different in that the  $\pi$ -electron acceptors are “hard”, strongly polarized NH bonds or alkali metal cations. Despite the potential biological relevance of this type of  $\pi$ -coordination, the literature contains only a scattering of essentially unconnected experimental studies with synthetic receptors.<sup>6–12</sup> An important contribution was recently made by Hay and co-workers who surveyed the crystallographic database and found evidence for directionality of hydrogen bonds to oxyanions.<sup>13</sup> More specifically, they showed that trigonal oxyanions (like  $\text{NO}_3^-$  and

**Scheme 2.** Hydrogen Bonding with Nitrate Lone Pair Electrons ( $\text{H}\cdots\text{O}-\text{N}-\text{O}$  Dihedral Angle is  $0^\circ$ ) is Favored over Hydrogen Bonding with  $\pi$ -Electrons ( $\text{H}\cdots\text{O}-\text{N}-\text{O}$  Dihedral Angle is  $90^\circ$ )



$\text{AcO}^-$ ) prefer to form hydrogen bonds with R–H acceptors that have  $\text{H}\cdots\text{O}-\text{A}$  angles near  $120^\circ$  and  $\text{H}\cdots\text{O}-\text{A}-\text{O}$  dihedral angles near  $0^\circ$ . In other words, the donor hydrogen atom lies within the plane of the trigonal anion. DFT calculations indicate that the hydrogen bond directionality is due to increased electrostatic potential at positions that correspond to the  $\text{sp}^2$  hybrid lone pairs on either side of the oxygen atoms. Hay calculates that the preference for hydrogen bonding to the oxygen lone pairs over the  $\pi$ -electron density is about 2 kcal/mol.<sup>14</sup>

The first part of this present study describes five X-ray structures that show subtle variations in receptor/salt complexation geometry. Of particular focus is a series of three  $\text{NO}_3^-$  salts where the exact orientation of the  $\text{NO}_3^-$  within the receptor cavity and the directionality of the hydrogen bonding ( $\pi$ -electrons versus lone pair electrons; see Scheme 2) vary with the identity of the counteranion. The X-ray structures provide an experimental context for gauging the relative impact that hydrogen bond directionality has on complexation geometry. The second half of this study describes NMR data for the receptor/salt complexes in solution. Unusual NMR shielding effects are observed, such as upfield movements of receptor NH signal upon salt complexation, apparently induced by the diamagnetic anisotropy of the trigonal oxyanions. This has prompted us to calculate the anisotropic shielding surface for the  $\text{NO}_3^-$  anion.

## Results and Discussion

**X-ray Analysis of Solid-State Structures.** A common procedure was employed to obtain single crystals of receptor **1** complexed with  $\text{KAcO}$ ,  $\text{NaNO}_3$ ,  $\text{KNO}_3$ ,  $\text{LiNO}_3$ , or  $\text{NaNO}_2$ . The solid salt was first extracted into a solution of the receptor in  $\text{CDCl}_3$ , and then after receptor saturation, the solvent was decanted, evaporated, and the residue recrystallized (typically from ethyl acetate).<sup>15</sup> X-ray diffraction data were collected at low temperature and refined by standard methods. In most cases, there was some disorder in the crown ether region of the receptor due to conformational flexibility; however, the isophthalamide region was always well-resolved. To help the reader, the intramolecular distances and angles that are discussed in the next two paragraphs are also listed in Table 1.

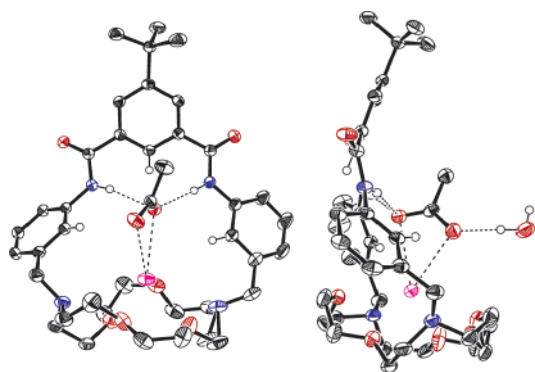
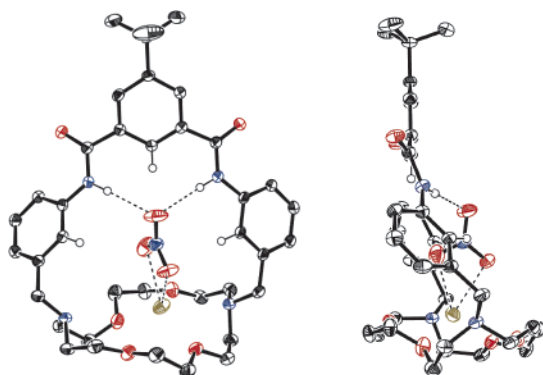
The X-ray crystal structure of **1**• $\text{KAcO}$  is shown in Figure 1. The  $\text{AcO}^-$  perches on the periphery of the macrobicyclic cavity and chelates the  $\text{K}^+$  cation which is located in the crown ether. The receptor NHs are directed toward one of the chelating oxygens, and the two intermolecular  $\text{N}\cdots\text{O}$  distances are 3.014(2) and 2.931(2) Å. The two  $\text{H}\cdots\text{O}-\text{C}-\text{O}$  dihedral angles

- (4) For reviews that discuss ditopic salt-binding receptors, see: (a) Gale, P. A. *Coord. Chem. Rev.* **2003**, *240*, 191–221. (b) Gale, P. A.; Beer, P. D. *Angew. Chem., Int. Ed.* **2001**, *40*, 486–516. (c) Kirkovits, G.; Shriver, J. A.; Gale, P. A.; Sessler, J. L. *J. Inclusion Phenom. Macrocyclic Chem.* **2001**, *41*, 69–75. For recent papers on ditopic salt-binding receptors, see: (d) Liu, Y.; Yang, Y. W.; Li, L.; Chen, Y. *Org. Biomol. Chem.* **2004**, *2*, 1542–1548. (e) Turner, D. R.; Spencer, E. C.; Howard, J. A. K.; Tocher, D. A.; Steed, J. W. *Chem. Commun.* **2004**, 1352–1353. (f) Plieger, P. G.; Tasker, P. A.; Galbraith, S. G. *Dalton Trans.* **2004**, 313–318. (g) Pajewski, R.; Ferdani, R.; Schlessinger, P. H.; Gokel, G. W. *Chem. Commun.* **2004**, 160–161. (h) Webber, P. R. A.; Beer, P. D. *Dalton Trans.* **2003**, 2249–2252. (i) Tongraung, P.; Chantarasiri, N.; Tuntulani, T. *Tetrahedron Lett.* **2003**, *44*, 29–32. (j) de Silva, A. P.; McClean, G. D.; Pagliari, S. *Chem. Commun.* **2003**, 2010–2011. (k) Miyaji, H.; Collinson, S. R.; Prokes, I.; Tucker, J. H. R. *Chem. Commun.* **2003**, 64–65. (l) Mansikkamaki, H.; Nissinen, M.; Schilley, C. A.; Rissanen, K. *New J. Chem.* **2003**, *27*, 88–97. (m) Vivas-Reyes, R.; De Proft, F.; Biesemans, M.; Willem, R.; Geerlings, P. *Eur. J. Inorg. Chem.* **2003**, 1315–1324. (n) Tozawa, T.; Tachikawa, T.; Tokita, S.; Kubo, Y. *New J. Chem.* **2003**, *27*, 221–223. (o) Cametti, M.; Nissinen, M.; Cort, A. D.; Mandolini, L.; Rissanen, K. *Chem. Commun.* **2003**, 2420–2421. (p) Glenny, M. W.; Blake, A. J.; Wilson, C.; Schroder, M. *Dalton Trans.* **2003**, 1941–1951. (q) Akkus, N.; Campbell, J. C.; Davidson, J.; Henderson, D. K.; Miller, H. A.; Parkin, A.; Parsons, S.; Pleiger, P. G.; Swart, R. M.; Tasker, P. A.; West, L. C. *Dalton Trans.* **2003**, 1932–1940. (r) Coxall, R. A.; Lindoy, L. F.; Miller, H. A.; Parkin, A.; Parsons, S.; Tasker, P. A.; White, D. J. *Dalton Trans.* **2003**, 55–64. (s) Evans, A. J.; Beer, P. D. *Dalton Trans.* **2003**, 4451–4456. (t) Bourgeois, J.; Fujita, M.; Kawano, M.; Sakamoto, S.; Yamaguchi, K. *J. Am. Chem. Soc.* **2003**, *125*, 9260–9261. (u) Oh, J. M.; Cho, E. J.; Ryu, B. J.; Lee, Y. J.; Nam, K. C. *Bull. Korean Chem. Soc.* **2003**, *24*, 1538–1540. (v) Kotch, F. W.; Sidorov, V.; Lam, Y. F.; Kayser, K. J.; Li, H.; Kaucher, M. S.; Davis, J. T. *J. Am. Chem. Soc.* **2003**, *125*, 15140–15150. (w) Camiolo, S.; Coles, S. J.; Gale, P. A.; Hursthouse, M. B.; Tizzard, G. J. *Supramol. Chem.* **2003**, *15*, 231–234. (x) Albrecht, M.; Zauner, J.; Eisele, T.; Weis, P. *Synthesis* **2003**, *7*, 1105–1111. (y) Tumchareng, G.; Tuntulani, T.; Coles, S. J.; Hursthouse, M. B.; Kilburn, J. D. *Org. Lett.* **2003**, *5*, 4971–4974. (z) Atwood, J. L.; Szumna, A. *Chem. Commun.* **2003**, 940–941.
- (5) Foster, R. *Organic Charge-Transfer Complexes*; Academic Press: New York, 1969.
- (6) Olsher, U.; Hankins, M. G.; Kim, Y. D.; Bartsch, R. A. *J. Am. Chem. Soc.* **1993**, *115*, 3370–3371. (b) Olsher, U.; Feinburg, H.; Frolow, F.; Shoham, G. *Pure Appl. Chem.* **1996**, *68*, 1195–1199.
- (7) Fräuter, G.; Weller, F.; Dehnicke, K. *Z. Naturforsch., B* **1989**, *44*, 444–454.
- (8) Steed, J. W.; Junk, P. C. *J. Chem. Soc., Dalton Trans.* **1999**, 2141–2146.
- (9) Koritsanszky, T.; Buschmann, J.; Luger, P.; Knochel, A.; Patz, M. *J. Am. Chem. Soc.* **1994**, *116*, 6748–6756.
- (10) Bisson, A. P.; Lynch, V. M.; Monahan, M. C.; Anslyn, E. V. *Angew. Chem., Int. Ed.* **1997**, *36*, 2340–2342. (b) Szumna, A.; Jurczak, J. *Eur. J. Org. Chem.* **2001**, 4031–4039.
- (11) Papoyan, G.; Gu, K.; Wiorcikiewicz-Kuczera, J.; Kuczera, K.; Bowman-James, K. *J. Am. Chem. Soc.* **1996**, *118*, 1354–1364. (b) Wiorcikiewicz-Kuczera, J.; Kuczera, K.; Bazzicalupi, C.; Bencini, A.; Valtancoli, B.; Bianchi, A.; Bowman-James, K. *New J. Chem.* **1999**, *23*, 1007–1013.
- (12) Mason, S.; Clifford, T.; Seib, L.; Kuczera, K.; Bowman-James, K. *J. Am. Chem. Soc.* **1998**, *120*, 8899–8900. (b) Clifford, T.; Danby, A.; Llinares, J. M.; Mason, S.; Alcock, N. W.; Powell, D.; Aguilera, J. A.; Garcia-Espana, E.; Bowman-James, K. *Inorg. Chem.* **2001**, *40*, 4710–4720. (c) Hynes, M. J.; Maubert, B.; Mckee, V.; Town, R. M.; Nelson, J. J. *Chem. Soc., Dalton Trans.* **2000**, 2853–2859.
- (13) Hay, B. P.; Dixon, D. A.; Bryan, J. C.; Moyer, B. A. *J. Am. Chem. Soc.* **2002**, *124*, 182–183.
- (14) Hay, B. P.; Gutowski, M.; Dixon, D. A.; Garza, J.; Rubicelia, R.; Moyer, B. A. *J. Am. Chem. Soc.* **2004**, *126*, 7925–7934.
- (15) The **1** salt complexes are typically quite soluble in chloroform, but they are insoluble in nonpolar hydrocarbons, such as toluene, and poorly soluble in oxygen-containing solvents, such as ethyl acetate, THF, and acetone.

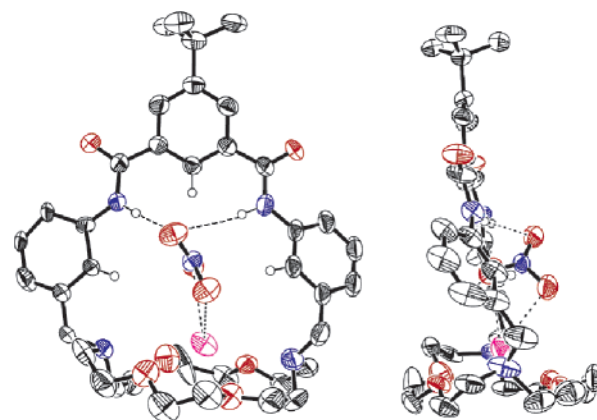
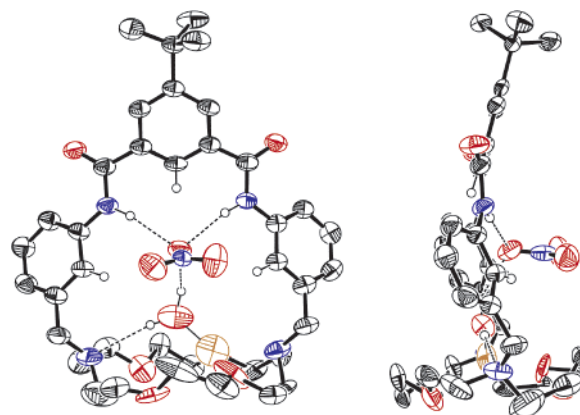
**Table 1.** Selected Solid-State Data for Receptor NH $\cdots$ Anion Interactions

	H $\cdots$ O–N–O dihedral angles <sup>a</sup>	N $\cdots$ O distances (Å)	N–H $\cdots$ O angles
<b>1</b> •KAcO	90 <sup>ob</sup> 28 <sup>ob</sup>	3.014(2) 2.931(2)	168° 175°
<b>1</b> •NaNO <sub>3</sub>	78° 34°	3.145(3) 3.235(3)	176° 177°
<b>1</b> •KNO <sub>3</sub> <sup>c</sup>	70° 15°	3.836(6) 2.903(5)	166° 160°
<b>1</b> •Li•2H <sub>2</sub> O•NO <sub>3</sub>	37° 28°	3.070(2) 3.031(2)	169° 170°

<sup>a</sup> Dihedral angle is defined in Scheme 2. <sup>b</sup> H $\cdots$ O–C–O dihedral angles. <sup>c</sup> Data for 70% occupancy structure.

**Figure 1.** Front and side views of the X-ray structure of [**1**•K<sup>+</sup>•AcO<sup>-</sup>•H<sub>2</sub>O].**Figure 2.** Front and side views of the X-ray crystal structure of [**1**•Na<sup>+</sup>•NO<sub>3</sub><sup>-</sup>]. Absent are solvent molecules in the lattice voids.

are 28 and 90°. The X-ray structure of **1**•NaNO<sub>3</sub> (Figure 2) shows that the NO<sub>3</sub><sup>-</sup> is located deep inside the macrocyclic cavity and chelates the bound Na<sup>+</sup>. The receptor NH residues form hydrogen bonds with the nonchelating NO<sub>3</sub><sup>-</sup> oxygen (the two intermolecular N $\cdots$ O distances are 3.145(3) and 3.235(3) Å, and the two H $\cdots$ O–N–O dihedral angles are 34 and 78°). In the case of solid-state **1**•KNO<sub>3</sub>, the larger K<sup>+</sup> cation forces the chelating NO<sub>3</sub><sup>-</sup> to sit further out of the receptor cavity, which gives the NO<sub>3</sub><sup>-</sup> more freedom to move. Indeed, the NO<sub>3</sub><sup>-</sup> flips between two unequally occupied positions between the two receptor NH residues. The 70% occupancy structure, shown in Figure 3, has two quite different intermolecular N $\cdots$ O distances to the nonchelating NO<sub>3</sub><sup>-</sup> oxygen (2.903(5) and 3.836(6) Å) and two quite different H $\cdots$ O–N–O dihedral angles of 15 and 70°. This asymmetrical positioning of the NO<sub>3</sub><sup>-</sup> allows the receptor to better align one of its two NH residues with the more basic lone pair electrons, thus forming a stronger hydrogen bond.

**Figure 3.** Front and side views of the X-ray crystal structure of [**1**•K<sup>+</sup>•NO<sub>3</sub><sup>-</sup>]. Absent are solvent molecules in the lattice voids. The 70% occupancy orientation is shown for nitrate.**Figure 4.** Front and side views of the X-ray crystal structure of [**1**•Li<sup>+</sup>•2H<sub>2</sub>O•NO<sub>3</sub><sup>-</sup>]. Absent is the second water molecule that is located underneath the crown and coordinated to the Li<sup>+</sup>.

The X-ray structure of the **1**•LiNO<sub>3</sub> complex (Figure 4) differs from those of the above sodium and potassium analogues in a number of ways. The Li<sup>+</sup> is coordinated by five heteroatoms, one nitrogen and two oxygens from the crown and two water oxygens (derived adventitiously from the atmosphere during the crystallization process). One of the water molecules bridges the cation and anion, a common feature in crystal structures of lithium salts complexed by macrocycles.<sup>16</sup> The receptor/NO<sub>3</sub><sup>-</sup> orientation is rotated almost 90°, compared to that of the sodium and potassium structures, which means that the receptor NH residues are directed primarily toward the two lone pairs on one of the NO<sub>3</sub><sup>-</sup> oxygens (the two intermolecular N $\cdots$ O distances are 3.070(2) and 3.031(2) Å, and the two H $\cdots$ O–N–O dihedral angles are 28 and 37°), and the bridging water OH is directed toward the NO<sub>3</sub><sup>-</sup> oxygen's  $\pi$ -electrons (H $\cdots$ O–N–O dihedral angle of 90°).<sup>17</sup> Thus, with these three receptor/NO<sub>3</sub><sup>-</sup> salt structures, the directionality of the hydrogen

(16) Olsher, U.; Izatt, R.; Bradshaw, J. S.; Dalley, N. K. *Chem. Rev.* **1991**, *91*, 137–164. (b) Boulatov, R.; Du, B.; Meyers, E. A.; Shore, S. G. *Inorg. Chem.* **1999**, *38*, 4554–4558. (c) Chivers, T.; Downard, A.; Parvez, M.; Schatte, G. *Inorg. Chem.* **2001**, *40*, 1975–1977.

(17) For other examples of hydrogen bonding to anion  $\pi$ -electrons, see: (a) Snowden, T. S.; Bisson, A. P.; Anslyn, E. V. *Bioorg. Med. Chem.* **2001**, *9*, 2467–2478. For rare examples of hydrogen bonding to the  $\pi$ -electrons of neutral molecules, see: (b) Liao, H.; Chu, S. *New J. Chem.* **2003**, *27*, 421–424. (c) Johnson, D. W.; Hof, F.; Iovine, P. M.; Nuckolls, C.; Rebek, J. *Angew. Chem., Int. Ed.* **2002**, *41*, 3793–3796. (d) Vachal, P.; Jacobson, E. N. *J. Am. Chem. Soc.* **2002**, *124*, 10012–10014.



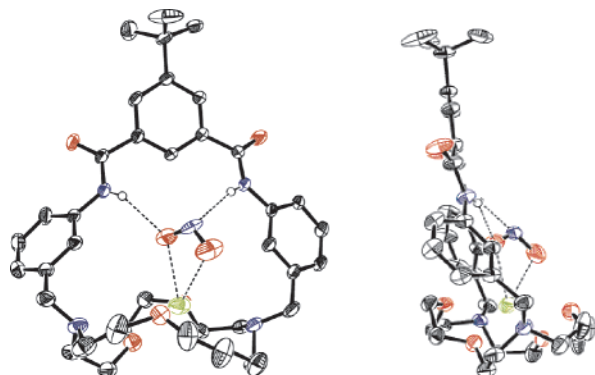


**Figure 5.** Front and side views of the X-ray crystal structure of  $[1\cdot\text{Na}^+\cdot\text{NO}_2^-]$ . Absent are solvent molecules in the lattice voids.

bonding between the complexed  $\text{NO}_3^-$  and the receptor NH is strongly influenced by the identity of the counteranion.

The last crystal structure to be discussed is  $1\cdot\text{NaNO}_2$ . Although  $\text{NO}_2^-$  is an anion of biological, environmental, and synthetic significance,<sup>18</sup> it is rarely included in studies of anion binding by synthetic receptors. The molecular recognition of  $\text{NO}_2^-$  is potentially a rich topic because it has not only an anisotropic shape but also an ambident coordination ability via the lone pairs on oxygen or on nitrogen.<sup>19</sup> The crystal structure of  $1\cdot\text{NaNO}_2$  (Figure 5) shows that the  $\text{NO}_2^-$  is chelated to the bound  $\text{Na}^+$  inside the macrocyclic cavity, but the anion does not sit symmetrically between the two NH residues. The  $\text{NO}_2^-$  nitrogen is closer to one of the receptor NH residues (intermolecular  $\text{N}\cdots\text{N}$  distances are 3.315(4) and 3.649(4) Å) which forces the hydrogen-bonded  $\text{NO}_2^-$  oxygen to be closer to the other NH residue (intermolecular  $\text{N}\cdots\text{O}$  distance is 2.903(4) Å with a  $\text{H}\cdots\text{O}-\text{N}-\text{O}$  dihedral angle of 33°). As discussed above, this asymmetrical positioning of the  $\text{NO}_2^-$  allows the receptor to better align its two NH residues with the anion's more basic lone pair electrons, thus forming stronger hydrogen bonds.

Taken together, the X-ray structures in Figures 1–5 provide a series of “snapshots” that illustrate how differences in the anisotropic shape of the trigonal oxyanion lead to subtle variations in receptor/salt complexation geometry in the solid state. It appears that anion orientation is controlled by a subtle interplay of steric factors (including crystal packing forces), coordination bonding to the simultaneously bound counteranion, and hydrogen bonding to the receptor. This latter factor includes a modest preference to direct the two receptor NH residues toward the more basic oxyanion lone pairs. The directionality can be overwhelmed by stronger bonding effects, such as ion-pairing. For example, in four out of the five X-ray structures, the anion is directly chelated to the counter metal cation, but this is only achieved by twisting the receptor/anion orientation such that one or both of the receptor NH residues are pointing substantially at the anion's  $\pi$ -surface. This weaker hydrogen bonding arrangement is more than offset by the formation of strong coordination bonds with the metal cation. A more subtle feature with these four chelated structures is that the anion is not oriented symmetrically inside the receptor. Hydrogen

bonding strength has a sinusoidal dependence on the dihedral angle,<sup>14</sup> and so there is an overall energetic benefit to adopting a twisted orientation that allows one of the two receptor NH residues to align well with a lone pair of electrons on the anion.

**NMR Analysis of Solution-State Structures.** Treatment of solutions of **1** in  $\text{CDCl}_3$  with solid salts leads to slow solubilization of the salts until the receptor is saturated (Figure 6). Listed in Table 2 are the changes in  $^1\text{H}$  NMR chemical shifts for the receptor signals upon salt complexation. In the case of  $\text{NaCl}$ ,  $\text{NaAcO}$ , and  $\text{KAcO}$ , the NH signals move downfield 0.7–0.9 ppm, as expected.<sup>20</sup> On the other hand, complexation with the nitrate and nitrite salts induces quite different changes in chemical shift. In some cases, the NH signal moves *upfield* by 0.05–0.22 ppm. *To the best of our knowledge, an upfield shift of a neutral receptor amide NH signal upon anion complexation is unprecedented.*<sup>21</sup> Another unusual change is the large upfield shift of equivalent protons **c** (see Table 2 for a comparison of complexed-induced shifts). These unusual changes in chemical shift upon complexation indicate that the magnetic shielding environment around a trigonal oxyanion, like  $\text{NO}_3^-$ , is anisotropic. Indeed, as described below, we have calculated the shielding surface around the  $\text{NO}_3^-$  anion and find that it is deshielding around the peripheral plane of the molecule and shielding in a region above the central nitrogen.

Many published studies in supramolecular chemistry have employed complexation-induced changes in chemical shift as a method of elucidating supramolecular structures in solution. Although there remains some debate over the origin of anisotropic shielding effects,<sup>22</sup> there is little doubt about the empirical utility of the method, especially with aromatic organic guests. In the present case, the guests are salts with anisotropic trigonal oxyanions, and the question arises whether the complexation-induced changes in chemical shifts that are listed in Table 2 can provide information concerning the structure of the receptor/salt complexes in solution. In some cases, the solution-state NMR data seem to match the data of the solid-state structure. For example, the signals for the NH and **c** protons in **1** move upfield by –0.22 and –0.18 ppm, respectively, when **1** is saturated with  $\text{NaNO}_3$ , and the X-ray structure of  $1\cdot\text{NaNO}_3$  suggests that this is because the NH and **c** protons are located in shielding zones above and below the plane of the encapsulated  $\text{NO}_3^-$ .

When **1** is saturated with  $\text{LiNO}_3$ , the solution-state NMR data do not appear to match with those of the solid-state structure. For example, the receptor NH and **c** protons move upfield by –0.22 and –0.09 ppm, respectively, but the X-ray structure of  $1\cdot 2\text{H}_2\text{O}\cdot\text{LiNO}_3$  shows that the NH and **c** protons are located in the peripheral plane around the encapsulated  $\text{NO}_3^-$  (deshielding zones). This suggests that the X-ray structure is not the predominant structure in solution. Evidence in favor of this hypothesis was gained from a variable temperature  $^1\text{H}$  NMR study of the complex. The system undergoes dynamic exchange

- (18) Rubio, M. A.; Lissi, E.; Villena, G. *Atmos. Environ.* **2002**, *36*, 293–297. (b) Jackson, M. A.; Tiedje, J. M.; Averill, B. A. *FEBS Lett.* **1991**, *291*, 41–44. (c) Bhati, N.; Kabra, A.; Narang, C. K.; Mathur, N. K. *J. Org. Chem.* **1991**, *56*, 4967–4969.
- (19) Halfen, J.; Mahapatra, S.; Wilkinson, E. C.; Gengenbach, A. J.; Young, V. G.; Que, L.; Tolman, W. B. *J. Am. Chem. Soc.* **1996**, *118*, 763–776. (b) McKee, V.; Nelson, J.; Town, R. M. *Chem. Soc. Rev.* **2003**, *32*, 309–325.

(20) Konrat, R.; Tollinger, M.; Kontaxis, G.; Kräutler, B. *Monatsh. Chem.* **1999**, *130*, 961–982.

(21) The same upfield movement in NH chemical shift is observed when the solvent is changed to toluene, indicating that the shielding effect is independent of solvent structure. Upfield chemical shifts do sometimes occur when a guest anion displaces another anion from a cationic receptor. See, for example: Magrans, J. O.; Ortiz, A. R.; Molins, M. A.; Lebouille, P. H. P.; Sanchez-Quesada, J.; Prados, P.; Pons, M.; Gago, F.; deMendoza, J. *Angew. Chem., Int. Ed. Engl.* **1996**, *35*, 1712–1715.

(22) Wannere, C. S.; Schleyer, P. v. R. *Org. Lett.* **2003**, *5*, 605–608. (b) Viglione, R. G.; Zanasi, R. *Org. Lett.* **2004**, *6*, 2265–2267.

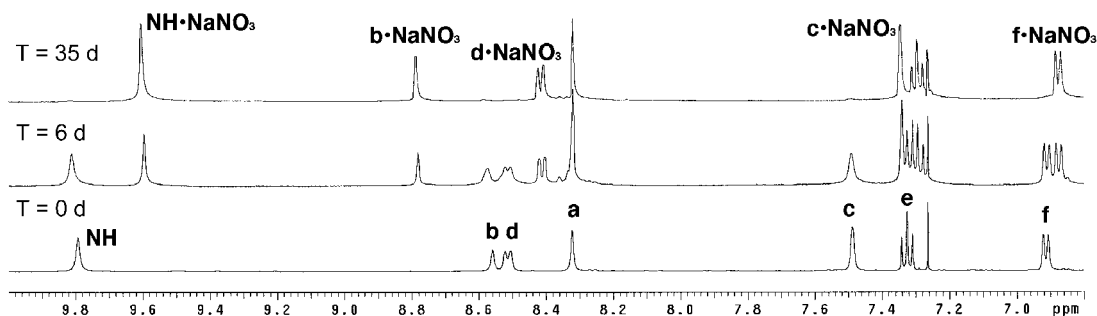


**Figure 6.** Partial  $^1\text{H}$  NMR spectra of receptor **1** in  $\text{CDCl}_3$  at 295 K after addition of solid  $\text{NaNO}_3$ . See structure of **1** for proton labeling.

**Table 2.** Change in  $^1\text{H}$  NMR Chemical Shift ( $\Delta\delta$ ) of Selected Protons upon Saturation of **1** with Salt<sup>a</sup>

salt	$\Delta\delta$ (ppm) <sup>b</sup>			
	a	b	NH	c
NaCl	+0.02	+0.66	+0.94	+0.87
NaAcO	0.00	+0.45	+0.72	+0.11
KAcO	-0.03	+0.48	+0.87	+0.05
$\text{NaNO}_3$	0.00	+0.21	-0.22	-0.18
$\text{KNO}_3$	0.00	+0.32	-0.05	-0.21
$\text{LiNO}_3$	-0.01	+0.20	-0.22	-0.09
$\text{NaNO}_2$	0.00	+0.21	-0.12	-0.13
$\text{KNO}_2$	0.00	+0.32	+0.31	-0.20
$\text{Bu}_4\text{NNO}_3^c$	-0.03	+0.04	+0.51	+0.27

<sup>a</sup> Solid salt extracted into solution of **1** (10 mM) in  $\text{CDCl}_3$  at  $T = 295$  K. <sup>b</sup> See structure of **1** for proton labeling;  $\Delta\delta = \delta \mathbf{1}\cdot\text{salt} - \delta \mathbf{1}$ . <sup>c</sup> Data obtained after mixing 150 mM  $\text{Bu}_4\text{NNO}_3$  and 10 mM **1** in  $\text{CDCl}_3$ .

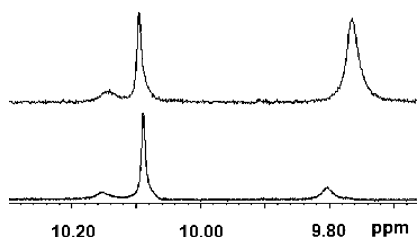


**Figure 7.** Partial  $^1\text{H}$  NMR spectrum of **1**· $\text{LiNO}_3$  at 213 K. Top: sample prepared by solid/liquid extraction using freshly opened  $\text{CDCl}_3$ . Bottom: sample prepared with water-saturated  $\text{CDCl}_3$ .

because at low temperature the spectrum splits into three sets of signals. Shown in Figure 7 are the signals for the NH residues at 213 K. The NH peak at 10.09 ppm corresponds to free receptor;<sup>23</sup> whereas the upfield peak at around 9.8 ppm is attributed to a dehydrated **1**· $\text{LiNO}_3$  complex with a structure that is analogous to that of **1**· $\text{NaNO}_3$  in Figure 2 (i.e., the  $\text{NO}_3^-$  is chelated to the  $\text{Li}^+$  inside the cavity of the receptor<sup>24</sup>). The downfield NH peak at 10.15 ppm is attributed to a hydrated complex with a structure that is very similar to that of **1**· $2\text{H}_2\text{O}\cdot\text{LiNO}_3$  in Figure 4. The relative ratio of these three signals depends on the amount of water in the sample. As depicted in Figure 7, the peak at 9.8 ppm (corresponding to dehydrated salt complex with chelated  $\text{LiNO}_3$ ) is diminished when water is added to the sample.

(23) At 213 K, a sample of free receptor exhibits an NH signal at 10.09 ppm. An alternative complex that has the receptor occupied only by a  $\text{Li}^+$  in the crown ether region is ruled out because a sample of receptor plus  $\text{LiClO}_4$  produces a new NH signal at 9.55 ppm at 213 K. Presumably, this signal is due to a receptor occupied only by  $\text{Li}^+$  and not the noncompetitive  $\text{ClO}_4^-$  anion.

(24) For examples of X-ray structures showing  $\text{NO}_3^-$  directly chelated to a  $\text{Li}^+$  that is encapsulated by a crown ether, see: Holt, E. M.; Malpass, G. D.; Ghirardelli, R. G.; Palmer, R. A.; Rubin, B. *Acta Crystallogr., Sect. C* **1984**, *40*, 394 and 396.

We conclude that the large complexation-induced changes in the  $^1\text{H}$  chemical shift for the protons that line the cavity of the receptor are strong evidence that the salts bind to the receptor cavity in solution.<sup>25</sup> In principle, the direction and magnitude of the shieldings can be used to elucidate the relative orientation of the encapsulated anisotropic anion; however, this requires quantitative mapping of the shielding surface around the anion (see below) and knowledge of the receptor/salt dynamics.<sup>26</sup> In certain cases (e.g., the **1**· $\text{LiNO}_3$  system above), the signal averaging due to dynamic exchange can be eliminated by acquiring the NMR spectrum at low temperature.

**Nitrate Shielding Surface.** The complexation-induced changes in the chemical shift described above are consistent with anisotropic shielding around the trigonal oxyanion. To the best of our knowledge, the shielding surface for a trigonal oxyanion, like  $\text{NO}_3^-$ , has not been reported.<sup>27,28</sup> Therefore, we calculated the  $\text{NO}_3^-$  shielding surface using density functional theory.

Textbook shielding surfaces are derived from McConnell's magnetic anisotropy or absolute shielding calculations for an isolated molecule. However, Martin and co-workers have recently shown that a probe nucleus will perturb the electronic structure of the molecule sufficiently to modify the predicted chemical shielding effects at the probe.<sup>29</sup> For simplicity, we used a helium nucleus as a probe and computed changes in the absolute shielding. As shown in Figure 8, unique values for the magnetic shielding in the vicinity of the  $\text{NO}_3^-$  are found in a hemispherical wedge, with the sphere centered on the nitrogen and one edge running along an N–O bond while the other bisects the adjacent O–N–O angle. In the molecular plane, the changes in chemical shift from the bare isolated atomic helium

(25) A referee suggests that it would be interesting to know the stability constants for salt binding to **1** in nonpolar solvents, and we agree. However, it would be extremely difficult to determine these values because of the very poor solubility of the sodium and potassium salts, which prohibits direct titration studies, and as discussed in ref 3c, competitive solid/liquid extraction studies strongly favor the lithium salts not because they necessarily have a stronger affinity but because they are inherently more soluble.

(26) It is intriguing to compare our  $\text{NaNO}_3$  complexation results to those of Anslin,<sup>10a</sup> whose related isophthalamide-based receptor is proposed to bind  $\text{NO}_3^-$  in a similar  $\pi$ -orientation, but nonetheless, downfield changes in receptor NH signals are produced upon  $\text{NO}_3^-$  complexation. Since the  $\text{NO}_3^-$  diamagnetic anisotropy has a steep dependency on spatial position, a possible explanation is that the Anslin receptor cavity is slightly too large for the  $\text{NO}_3^-$  guest and so the  $\text{NO}_3^-$  "rattles around" inside the receptor; thus, the receptor NH protons sense an average magnetic environment that is deshielding. This emphasizes the point that it is the sum of the various shielding factors that determines the NH chemical shift.

(27) Nitrate anisotropy is measured by NMR parameters, such as  $^{15}\text{N}$  shielding tensor and  $^{14}\text{N}$  quadrupole coupling constant: Mason, J.; Larkworthy, L. F.; Moore, E. A. *Chem. Rev.* **2002**, *102*, 913–934.

(28) For a summary of the diamagnetic anisotropy of the nitro group, see: Jackman, L. M.; Sternell, S. *Applications of Nuclear Magnetic Resonance Spectroscopy in Organic Chemistry*, 2nd ed.; Pergamon: Oxford, 1969; p 94.

(29) Martin, N. H.; Brown, J. D.; Nance, K. H.; Schaefer, H. F.; Schleyer, P. v. R.; Wang, Z. X.; Woodcock, H. L. *Org. Lett.* **2001**, *3*, 3823–3826.

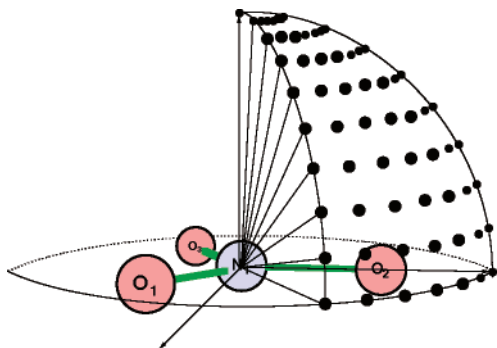


**Figure 8.** Unique locations on the nitrate shielding surface at a fixed distance from the nitrogen.

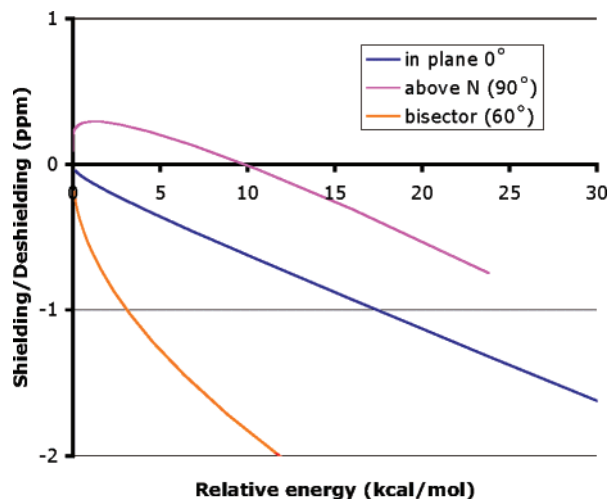


**Figure 9.** Variation in shielding at He as the probe approaches  $\text{NO}_3^-$  along three directions (see text).

value are downfield (i.e., the probe is deshielded). Only directly above the nitrogen ( $\pm 20^\circ$ ) is the probe shielded, although as it approaches close enough (less than  $\sim 1.85 \text{ \AA}$ ), deshielding again ensues. Figure 9 displays the variation in shielding at He as the probe approaches  $\text{NO}_3^-$  along three directions. For a given energy, approach toward the O along the N–O bond extension (blue) is deshielding, but the most deshielded approach is along the O–N–O bisector (orange). Approach from above the central nitrogen (magenta) goes through a shielded region, but the probe eventually becomes deshielded again at close approach.

## Summary

With trigonal oxyanions, such as  $\text{AcO}^-$  and  $\text{NO}_3^-$ , it is predicted that hydrogen bonding with the anion's lone pair electrons is about 2 kcal/mol stronger than with the  $\pi$ -electrons (Scheme 2).<sup>13</sup> However, this directionality preference is just one of several noncovalent factors that determine the binding orientation of a trigonal oxyanion encapsulated inside a receptor cavity. The solid-state receptor/salt structures described here indicate that anion orientation is controlled by a complex interplay of steric factors, coordination bonding to the metal cation, and hydrogen bonding to the receptor. The solution-state  $^1\text{H}$  NMR spectra of the nitrate and nitrite salt complexes are noteworthy because several receptor signals, including the NH protons, undergo unusual upfield movements in chemical shift upon complexation. This long-range shielding effect is attributed to the diamagnetic anisotropy of these trigonal oxyanions. The shielding surface for the  $\text{NO}_3^-$  anion is

calculated using density functional theory and is shown to have a shielding region directly above the central nitrogen.

## Experimental Section

**X-ray Crystal Data for  $1\cdot\text{KAcO}$ .** Crystals were obtained upon slow diffusion of hexane vapor into an ethyl acetate solution:  $\text{C}_{40}\text{H}_{53}\text{N}_4\text{K}_8\text{O}_8$ , monoclinic,  $P2_1/n$ ,  $a = 14.3976(7) \text{ \AA}$ ,  $b = 20.3199(9) \text{ \AA}$ ,  $c = 14.8154(7) \text{ \AA}$ ,  $\alpha = 90^\circ$ ,  $\beta = 112.971(1)^\circ$ ,  $\gamma = 90^\circ$ ,  $V = 3990.7(3) \text{ \AA}^3$ ,  $Z = 4$ ,  $T = 100(2) \text{ K}$ ,  $\mu(\text{Mo K}\alpha) = 0.192 \text{ mm}^{-1}$ ,  $D_{\text{calcd}} = 1.287 \text{ mg/m}^3$ ,  $R1 (I > 2\theta(I)) = 4.81\%$ ,  $wR2 (\text{all data}) = 14.41\%$  for 9178 independent reflections. The asymmetric unit contained a macrocycle with bound potassium acetate and one hydrogen-bonded water molecule. Two disordered portions of the aza-crown ether ring were refined as 60%/40% relative occupancies of O1–C3/O1A–C3A and 65%/35% occupancies of C6/C6A. The X-ray crystal data can be retrieved from the Cambridge Crystallographic Data Center using the deposition number CCDC 196909.

**X-ray Crystal Data for  $1\cdot\text{NaNO}_3$ .** Crystals were obtained upon slow evaporation of an ethyl acetate solution:  $\text{C}_{38}\text{H}_{50}\text{N}_5\text{NaO}_9$ , triclinic,  $P\bar{1}$ ,  $a = 13.2057(6) \text{ \AA}$ ,  $b = 13.2493(7) \text{ \AA}$ ,  $c = 13.4351(7) \text{ \AA}$ ,  $\alpha = 74.552(1)^\circ$ ,  $\beta = 74.532(1)^\circ$ ,  $\gamma = 73.806(1)^\circ$ ,  $V = 2128.34(19) \text{ \AA}^3$ ,  $Z = 2$ ,  $T = 100(2) \text{ K}$ ,  $\mu(\text{Mo K}\alpha) = 0.100 \text{ mm}^{-1}$ ,  $D_{\text{calcd}} = 1.271 \text{ mg/m}^3$ ,  $R1 (I > 2\theta(I)) = 7.23\%$ ,  $wR2 (\text{all data}) = 22.33\%$  for 10 576 independent reflections. The asymmetric unit contained one macrocycle with an associated sodium nitrate ion-pair, as well as disordered ethyl acetate solvent. The solvent was refined in two positions of 40% occupancy each (both positions also are 2-fold disordered), for a total of 0.8 solvent molecule per asymmetric unit. The solvent was refined isotropically, with no hydrogen atoms added. The X-ray crystal data can be retrieved from the Cambridge Crystallographic Data Center using the deposition number CCDC 188060.

**X-ray Crystal Data for  $1\cdot\text{KNO}_3$ .** Crystals were obtained upon slow evaporation of a dioxane solution:  $\text{C}_{38}\text{H}_{50}\text{N}_5\text{KO}_9$ , monoclinic,  $P2_1/n$ ,  $a = 11.0352(5) \text{ \AA}$ ,  $b = 13.6633(6) \text{ \AA}$ ,  $c = 27.7361(13) \text{ \AA}$ ,  $\alpha = 90^\circ$ ,  $\beta = 98.894(1)^\circ$ ,  $\gamma = 90^\circ$ ,  $V = 4131.7(3) \text{ \AA}^3$ ,  $Z = 4$ ,  $T = 100(2) \text{ K}$ ,  $\mu(\text{Mo K}\alpha) = 0.190 \text{ mm}^{-1}$ ,  $D_{\text{calcd}} = 1.292 \text{ mg/m}^3$ ,  $R1 (I > 2\theta(I)) = 8.13\%$ ,  $wR2 (\text{all data}) = 22.83\%$  for 7265 independent reflections. The asymmetric unit contains a macrocycle with an associated  $\text{KNO}_3$  ion-pair and one-half of a dioxane molecule. The nitrate occupies two positions within the host (70%/30%). The 70% occupancy structure is shown in Figure 5. The 30% occupancy structure has nearly identical intermolecular  $\text{N}\cdots\text{O}$  distances, but the upper nitrate oxygen is pointed toward the other amide. Most of the crown unit is 2-fold disordered (58%/42% occupancies), along with one of the connected phenyl groups. The disordered phenyl rings were refined as regular hexagons. The *tert*-butyl substituent exhibits a 2-fold rotational disorder (80%/20% occupancies). Both amide oxygen atoms are also disordered (55%/45% and 63%/37% occupancies for O5 and O6, respectively). One carbon atom in the dioxane half-molecule is also disordered (72%/28% occupancies). All disordered positions were anisotropically refined, with disordered hydrogen atoms' positions also assigned. The X-ray crystal data can be retrieved from the Cambridge Crystallographic Data Center using the deposition number CCDC 196910.

**X-ray Crystal Data for  $1\cdot\text{Li}\cdot 2\text{H}_2\text{O}\cdot\text{NO}_3$ .** Crystals were obtained upon slow evaporation of an ethyl acetate solution:  $\text{C}_{38}\text{H}_{54}\text{LiN}_5\text{O}_{11}$ , triclinic,  $P\bar{1}$ ,  $a = 10.785(2) \text{ \AA}$ ,  $b = 13.577(3) \text{ \AA}$ ,  $c = 14.016(3) \text{ \AA}$ ,  $\alpha = 87.596(4)^\circ$ ,  $\beta = 79.170(4)^\circ$ ,  $\gamma = 76.860(4)^\circ$ ,  $V = 1962.8(8) \text{ \AA}^3$ ,  $Z = 2$ ,  $T = 100(2) \text{ K}$ ,  $\mu(\text{Mo K}\alpha) = 0.095 \text{ mm}^{-1}$ ,  $D_{\text{calcd}} = 1.292 \text{ mg/m}^3$ ,  $R1 (I > 2\theta(I)) = 10.88\%$ ,  $wR2 (\text{all data}) = 33.81\%$  for 15 480 independent reflections. The asymmetric unit contains a macrocycle with an associated  $\text{LiNO}_3$  ion-pair and two water molecules bound to the lithium ion. Most of the crown unit is 2-fold disordered (50%/50% occupancies). All disordered positions were anisotropically refined, with disordered hydrogen atoms' positions also assigned. The X-ray crystal data can be retrieved from the Cambridge Crystallographic Data Center using the deposition number CCDC 250320.



**X-ray Crystal Data for 1•NaNO<sub>2</sub>.** Crystals were obtained upon slow evaporation of an ethyl acetate solution: C<sub>38</sub>H<sub>50</sub>N<sub>5</sub>NaO<sub>8</sub>•0.68-(C<sub>4</sub>H<sub>8</sub>O<sub>2</sub>), triclinic, *P* $\bar{1}$ , *Z* = 4, *a* = 13.1842(2) Å, *b* = 13.3913(2) Å, *c* = 25.3011(5) Å,  $\alpha$  = 76.996°,  $\beta$  = 77.410°,  $\gamma$  = 72.797°, *V* = 4102.34 Å<sup>3</sup>,  $\mu$ (Mo K $\alpha$ ) = 0.7107 mm<sup>-1</sup>, *D*<sub>calcd</sub> = 1.276 mg/m<sup>3</sup>, *R*1 (*I* > 2 $\theta$ (*I*)) = 8.21%, *wR*2 (all data) = 23.07% for 14 452 observed independent reflections (*R* factors based on *F*<sup>2</sup> rather than *F* give values about 2-fold larger than those based on *F*). Hydrogens bound to carbon were placed at calculated geometries and allowed to ride the position of the parent atom. Hydrogen parameters were set to 1.2 times the equivalent isotropic U of the parent atom, 1.5 times for methyl hydrogens. Hydrogens bound to nitrogen were located from a difference Fourier map. There were two independent molecules and two disordered ethyl acetates in the asymmetric unit, giving a molecular formula of C<sub>38</sub>H<sub>50</sub>N<sub>5</sub>NaO<sub>8</sub>•0.68(C<sub>4</sub>H<sub>8</sub>O<sub>2</sub>). Several atom sites in the two independent molecules were determined to contain an element of disorder. The occupancies were refined as pairs that summed to a value of 100% occupancy. O1 had a major position with site occupancy of 72(0)%, and C39 had the major position 69.1(11)% occupied. Disorder was also observed in one of the NaNO<sub>2</sub> salts where N10 had its major position occupied 53(4)% and O16 was resolved at 75.2(11)% occupancy. The X-ray crystal data can be retrieved from the Cambridge Crystallographic Data Center using the deposition number CCDC 250321.

**Computational Details.** The structure of the free nitrate ion was optimized, assuming *D*<sub>3h</sub> molecular symmetry, using a density functional theory (DFT) approach and a flexible basis set of approximately triple- $\zeta$  quality,<sup>30</sup> augmented with a set of diffuse sp functions<sup>31</sup> and multiple polarization functions.<sup>32</sup> This basis can be denoted 6-311+G(2d). Nuclear shielding in the vicinity of the nitrate ion was evaluated by computing the chemical shift at a helium atom, probing unique locations in the surrounding space. In these calculations, the GIAO approach was adopted.<sup>33</sup> With the above combination of theoretical model and basis set, but also including p functions, the absolute shielding at a

bare helium atom is 59.93 au. Calculations at this level have been shown to provide a satisfactory description of nuclear shielding tensors in many molecular environments.<sup>34</sup> Both the Gaussian03<sup>35</sup> and a local version of the Dalton<sup>36</sup> electronic structure programs were employed, and the B3LYP functional<sup>37</sup> was used throughout.

**Acknowledgment.** This work was supported by the University of Notre Dame and the National Science Foundation. The Notre Dame Radiation Laboratory is supported by the Office of Basic Energy Sciences of the United States Department of Energy. This is Document No. NDRL- 4556 from the Notre Dame Radiation Laboratory.

**Supporting Information Available:** X-ray data as CIFs. This material is available free of charge via the Internet at <http://pubs.acs.org>.

JA0440295

- (30) Krishnan, R.; Binkley, J. S.; Seeger, R.; Pople, J. A. *J. Chem. Phys.* **1980**, *72*, 650–654.  
(31) Clark, T.; Chandrasekhar, J.; Spitznagel, G. W.; Schleyer, P. v. R. *J. Comput. Chem.* **1983**, *4*, 294–301.  
(32) Frisch, M. J.; Pople, J. A.; Binkley, J. S. *J. Chem. Phys.* **1984**, *80*, 3265–3269.

- (33) Wolinski, K.; Hinton, J. F.; Pulay, P. *J. Am. Chem. Soc.* **1990**, *112*, 8251–8260.  
(34) Cheeseman, J. R.; Trucks, G. W.; Keith, T. A.; Frisch, M. J. *J. Chem. Phys.* **1996**, *104*, 5497–5509.  
(35) Frisch, M. J.; Trucks, G. W.; Schlegel, H. B.; Scuseria, G. E.; Robb, M. A.; Cheeseman, J. R.; Montgomery, J. A., Jr.; Vreven, T.; Kudin, K. N.; Burant, J. C.; Millam, J. M.; Iyengar, S. S.; Tomasi, J.; Barone, V.; Mennucci, B.; Cossi, M.; Scalmani, G.; Rega, N.; Petersson, G. A.; Nakatsuji, H.; Hada, M.; Ehara, M.; Toyota, K.; Fukuda, R.; Hasegawa, J.; Ishida, M.; Nakajima, T.; Honda, Y.; Kitao, O.; Nakai, H.; Klene, M.; Li, X.; Knox, J. E.; Hratchian, H. P.; Cross, J. B.; Adamo, C.; Jaramillo, J.; Gomperts, R.; Stratmann, R. E.; Yazyev, O.; Austin, A. J.; Cammi, R.; Pomelli, C.; Ochterski, J. W.; Ayala, P. Y.; Morokuma, K.; Voth, G. A.; Salvador, P.; Dannenberg, J. J.; Zakrzewski, V. G.; Dapprich, S.; Daniels, A. D.; Strain, M. C.; Farkas, O.; Malick, D. K.; Rabuck, A. D.; Raghavachari, K.; Foresman, J. B.; Ortiz, J. V.; Cui, Q.; Baboul, A. G.; Clifford, S.; Cioslowski, J.; Stefanov, B. B.; Liu, G.; Liashenko, A.; Piskorz, P.; Komaromi, I.; Martin, R. L.; Fox, D. J.; Keith, T.; Al-Laham, M. A.; Peng, C. Y.; Nanayakkara, A.; Challacombe, M.; Gill, P. M. W.; Johnson, B.; Chen, W.; Wong, M. W.; Gonzalez, C.; Pople, J. A. *Gaussian 03*, revision B.04; Gaussian, Inc.: Pittsburgh, PA, 2003.  
(36) Helgaker, T.; Jensen, H. J. A.; Jørgensen, P.; Olsen, J.; Ruud, K.; Ågren, H.; Auer, A. A.; Bak, K. L.; Bakken, V.; Christiansen, O.; Coriani, S.; Dahle, P.; Dalskov, E. K.; Enevoldsen, T.; Fernandez, B.; Hättig, C.; Hald, K.; Halkier, A.; Heiberg, H.; Hettema, H.; Jonsson, D.; Kirpekar, S.; Kobayashi, R.; Koch, H.; Mikkelsen, K. V.; Norman, P.; Packer, M. J.; Pedersen, T. B.; Ruden, T. A.; Sanchez, A.; Saue, T.; Sauer, S. P. A.; Schimmelpfennig, B.; Sylvester-Hvid, K. O.; Taylor, P. R.; Vahtras, O. *DALTON* (a molecular electronic structure program), release 1.2, 2001.  
(37) Becke, A. D. *J. Chem. Phys.* **1993**, *98*, 5648–5662.